ACADEMIC PRESS

Available online at www.sciencedirect.com

SCIENCE DIRECT®

DEVELOPMENTAL BIOLOGY

Developmental Biology 258 (2003) 169–184

www.elsevier.com/locate/ydbio

Tissue interactions pattern the mesenchyme of the embryonic mouse lung

Molly Weaver,[a] Lorene Batts,[b] and Brigid L.M. Hogan[a,b,*]

[a] *Department of Cell and Developmental Biology, Vanderbilt University Medical Center, Nashville, TN 37232-2175, USA*
[b] *Howard Hughes Medical Institute, Vanderbilt University Medical Center, Nashville, TN 37232-2175, USA*

Received for publication 9 January 2003, revised 14 February 2003, accepted 14 February 2003

Abstract

The mechanisms that control proliferation and differentiation of embryonic lung mesenchyme are largely unknown. We describe an explant system in which exogenous recombinant N-Sonic Hedgehog (N-Shh) protein sustains the survival and proliferation of lung mesenchyme in a dose-dependent manner. In addition, Shh upregulates several mesenchymal cell markers, including its target gene *Patched (Ptc)*, intercellular signaling genes *Bone Morphogenetic Protein-4 (Bmp4)* and *Noggin (Nog)*, and smooth muscle actin and myosin. In explants exposed to N-Shh in the medium, these products are upregulated throughout the mesenchyme, but not in the periphery. This exclusion zone correlates with the presence of an overlying mesothelial layer, which, as in vivo, expresses *Fibroblast Growth Factor 9 (Fgf9)*. Recombinant Fgf9 protein inhibits the differentiation response of the mesenchyme to N-Shh, but does not affect proliferation. We propose a model for how factors made by two epithelial cell populations, the inner endoderm and the outer jacket of mesothelium, coordinately regulate the proliferation and differentiation of the lung mesoderm.

Keywords: Lung; Mesenchyme; Smooth muscle; Bmp4; Noggin; Shh; Patched; Fgf9; Mesothelium; In vitro culture

Introduction

Reciprocal epithelial–mesenchymal interactions are essential for the growth, differentiation, and patterning of many vertebrate organs. One of these is the embryonic mouse lung, which has proved a valuable model system for studying the molecular basis of signaling between embryonic tissue layers. The lung arises from the ventral foregut at embryonic day 10 (E10) as two primary buds, each consisting of three cell layers: the inner epithelium (of endodermal origin), the surrounding mesenchymal stroma, and a thin outer mesothelium. Early in development, the epithelium undergoes a stereotypic pattern of branching morphogenesis that is dependent on signals from the mesenchyme. Considerable work has focused on the molecular mechanisms controlling this branching and the proximal–distal differentiation of the respiratory epithelium (reviewed in Cardoso, 2001; Hogan et al., 1997). By contrast, relatively little is known about tissue interactions regulating the development of the mesenchyme.

The cellular composition of the mesenchyme is complex and involves the distinct patterning of different cell types. One of the most obvious patterns is seen in smooth muscle, the development of which is temporally and spatially coordinated with that of the respiratory epithelium. At the level of the main bronchi, smooth muscle overlies the dorsal surface of the endoderm, while cartilaginous rings partially encompass the ventral airways. In all successive proximal airways, smooth muscle cells encircle the entire endoderm, but are characteristically absent from the advancing tips of distal airways during branching morphogenesis (Tollet et al., 2001). In addition to smooth muscle and cartilage, there is evidence that early distal mesenchyme gives rise to endothelial cells of blood vessels and pericytes by the process of vasculogenesis (deMello et al., 1997; Partanen et al.,

* Corresponding author. Department of Cell Biology, Box 3709, Duke University Medical Center, Durham, NC 27710, USA. Fax: +1-919-684-8592.
E-mail address: b.hogan@cellbio.duke.edu (B.L.M. Hogan).

0012-1606/03/$ – see front matter © 2003 Elsevier Science (USA). All rights reserved.
doi:10.1016/S0012-1606(03)00117-9

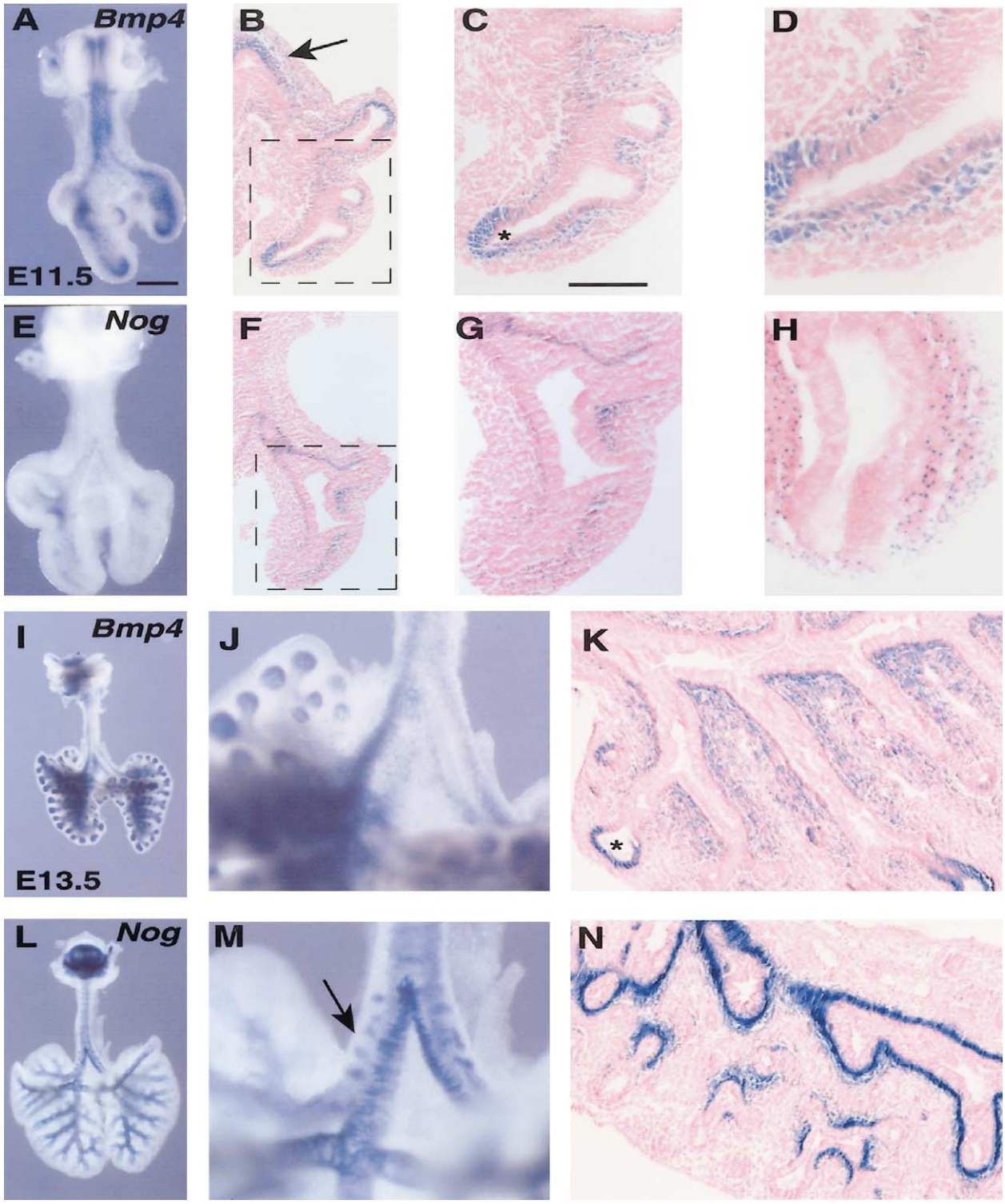

Fig. 1. *Bmp4*^{lacZ} and *Nog*^{lacZ} are expressed in overlapping domains in the lung mesenchyme. (A) Ventral view of *Bmp4*^{lacZ} expression in E11.5 lung. (B) Section through E11.5 *Bmp4*^{lacZ} lung. Note strong expression in mesenchyme cells adjacent to main bronchi (arrow), proximal endoderm, and in interbud regions. Boxed area shown at higher magnifications in (C) and (D). (E) Ventral view of *Nog*^{lacZ} expression in E11.5 lung. (F) Section through the same. Boxed area shown at higher magnification in (G). (G) *Nog*^{lacZ}-expressing cells are directly adjacent to the proximal epithelium and in interbud regions. (H) Low, "salt-and-pepper" staining of *Nog*^{lacZ}-positive cells in distal mesenchyme at E11.0. (I) Ventral view of *Bmp4*^{lacZ} lung at E13.5. (J) High magnification of main bronchi in (I). (K) Section through E13.5 *Bmp4*^{lacZ} lung. Note gradient of *Bmp4*^{lacZ} activity, with highest expression adjacent to epithelium decreasing toward periphery. (L) Ventral view of *Nog*^{lacZ} expression at E13.5 but slightly more advanced than in (I). (M) Main bronchi of lung shown in (L). Expression is seen in developing cartilage rudiments (arrow) and parabronchial smooth muscle. (N) Section through E13.5 *Nog*^{lacZ} lung. Expression restricted to cells directly adjacent to proximal epithelium. All sections counterstained with eosin. Asterisks in (C) and (K) indicate *Bmp4*^{lacZ} expression in distal epithelium. Scale bar in (A), 300 μm in (A, E, J, M); 800 μm in (I, L). Scale bar in (C), 200 μm in (C, G); 400 μm in (B, F, K, N); 100 μm in (D, H).

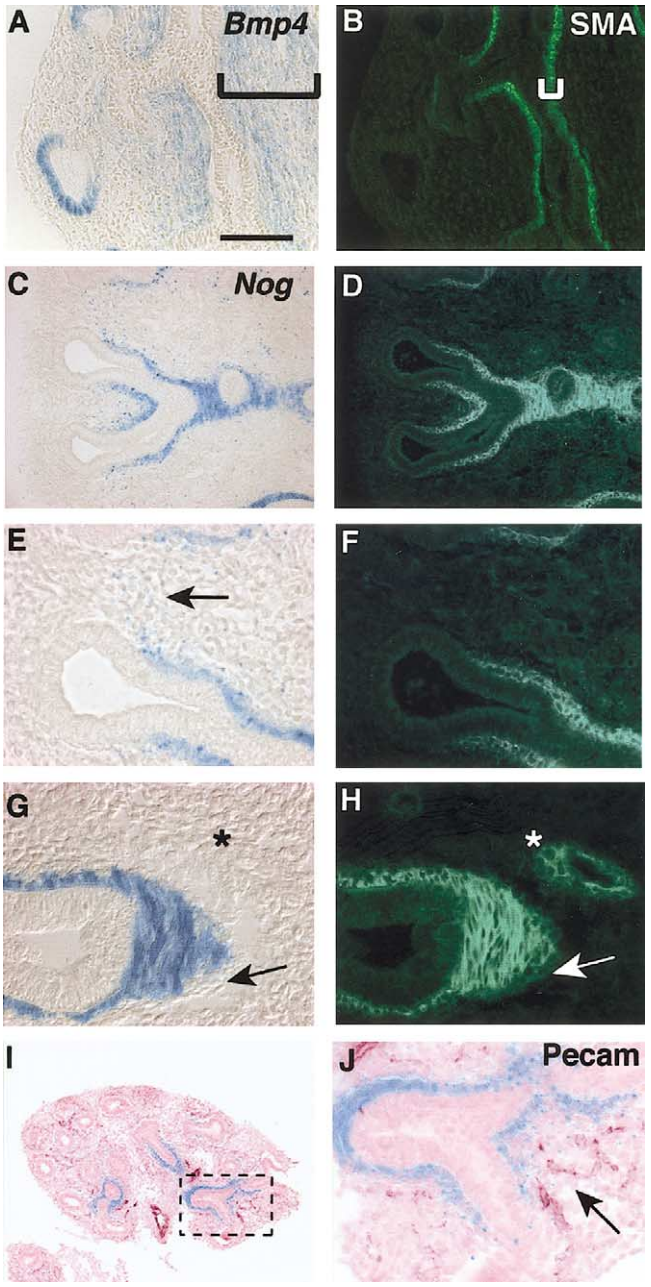

Fig. 2. Parabronchial smooth muscle cells coexpress Nog^{lacZ}, $Bmp4^{lacZ}$, and sma. (A) Nomarski bright-field of $Bmp4^{lacZ}$ activity (blue) in a wide domain of the lung mesenchyme (black bracket). (B) Sma is detected in a subset of $Bmp4^{lacZ}$-positive cells adjacent to the endoderm (white bracket). (C) Nog^{lacZ} expression. (D) Sma-expressing cells are confined to the Nog^{lacZ}-expressing cell layer. (E) High magnification of distal tip in (C). Note two populations of Nog^{lacZ}-expressing cells: smooth muscle adjacent to the proximal endoderm, and cells with a "salt-and-pepper" distribution more distally (arrow). (F) The first population coexpresses sma; the second does not. (G) Nomarksi image of Nog^{lacZ} proximal airway and adjacent blood vessel (*). (H) Only parabronchial smooth muscle is positive for Nog^{lacZ}. Both blood vessel-associated smooth muscle and parabronchial smooth muscle stain with sma. (I, J) Pecam antibody staining (purple) counterstained with eosin. Nog^{lacZ} cells (blue) do not colocalize with large vessels in proximal regions (I) or with capillaries in distal regions (J). Boxed region in (I) is shown at higher magnification in (J). All lungs are E13.5. Scale bar in (A), 400 μm in (A–D); 200 μm in (I); 800 μm in (E–H).

1996) and to artery-associated smooth muscle (Hall et al., 2000). Postnally, the distal mesoderm generates myofibroblasts in the tips of the alveolar septae (Bostrom et al., 1996; Kapanchi, 1997). Additional cell types found in the lung include stromal fibroblasts, interstitial lipofibroblasts (McGowan and Torday, 1997), and lymphatic vessels.

Insight into lung mesenchyme development comes from both cellular and genetic studies. Lung mesenchyme cultured in vitro in the absence of endoderm fails to undergo either morphogenesis or differentiation, even in the presence of 10% serum (Gebb and Shannon, 2000; Taderera, 1967). This suggests that the endoderm normally releases components required by lung mesenchyme, and several lines of genetic evidence point to Sonic hedgehog (N-Shh) as one factor involved. First, *Shh* is expressed in lung endoderm from the earliest stages of development, and protein is detected in respiratory epithelial cells from E10.5 until birth (Bellusci et al., 1997; Bitgood and McMahon, 1995; Miller et al., 2001). The gene encoding its receptor and downstream target, *Ptc*, is also transcribed in a dynamic pattern in the lung mesenchyme (Bellusci et al., 1997; Motoyama et al., 1998; this paper). Second, *Shh* homozygous null mutant mice have severely hypoplastic lungs; proliferation of the mesenchyme is reduced, and parabronchial smooth muscle differentiation is absent (Litingtung et al., 1998; Pepicelli et al., 1998). Third, transgenic overexpression of *Shh* in the endoderm leads to increased amounts of highly proliferative mesoderm (Bellusci et al., 1997). Finally, all three *Gli* genes (*Gli1*, *Gli2*, and *Gli3*) encoding downstream intracellular regulators of Shh signaling are expressed in overlapping domains in the mesoderm (Grindley et al., 1997; Hui et al., 1994; Platt et al., 1997). Embryos lacking combinations of *Gli* genes exhibit a spectrum of lung defects, ranging from abnormally shaped and fused lobes to complete absence of lung buds in $Gli2^{-/-}$; $Gli3^{-/-}$ compound mutants (Grindley et al., 1997; Motoyama et al., 1998; Park et al., 2000). Taken together, these phenotypes suggest that the Shh signaling pathway has multiple roles in mesenchymal cell proliferation, differentiation, and patterning.

There is evidence that another cell layer, the outer mesothelium, is also essential for lung mesenchymal development. Mutation of *Fibroblast growth factor 9 (Fgf9)*, expressed at high levels in the mesothelium, results in a decrease in stromal proliferation. Although the lung epithelium differentiates normally and the pulmonary vasculature is present, this loss of mesenchymal mass results in a smaller lung, with fewer generations of epithelial branches (Colvin et al., 1999, 2001). However, the precise mechanisms by which Fgf9 affects lung mesenchyme development remain largely unexplored.

Here, we have developed an explant system to examine the mechanisms controlling lung mesoderm survival, differentiation, and patterning. We show that N-Shh promotes mesenchymal cell proliferation, the expression of genes encoding several intercellular signaling factors, and the dif-

ferentiation of smooth muscle. By contrast, we demonstrate that Fgf9 produced by the mesothelium inhibits the upregulation of signaling factors and the differentiation of smooth muscle in response to Shh. Taken together, the results suggest a model for how the endoderm and the mesothelium cooperate in vivo to regulate the development of the intervening mesoderm.

Materials and methods

Embryos and mouse strains

Wildtype embryos were from ICR outbred mice (Harlan-Sprague-Dawley, Indianapolis, IN). Mice carrying the lacZ reporter alleles *Bmp4*^{lacZ}, *Nog*^{lacZ}, and *Flk1*^{lacZ} have been described (Lawson et al., 1999; McMahon et al., 1998; Shalaby et al., 1995). *Nog*^{lacZ} homozygotes were obtained by intercrossing.

Mesenchyme and endoderm isolation

E11.5 embryos (noon on the day of vaginal plug is E0.5) heterozygous for the *lacZ* reporter allele were genotyped by staining hindlimbs for β-galactosidase activity. Lungs were washed two times in Tyrode–Ringer's solution and incubated in pancreatin–trypsin solution (Hogan et al., 1994) for 7–9 min on ice. Mesenchyme and endoderm were then separated by using tungsten needles in DMEM with 5% fetal bovine serum. Tightly adherent mesothelium was not specifically removed during dissection although its disruption was inevitable.

Tissue recombinations and mesenchyme explants

Each explant consisted of the total mesenchyme distal to the primary bronchi from one E11.5 lung, cultured on an 8-μm Nucleopore track-etch filter (Whatman #110414, Clifton, NJ) floating on Schuger's mesenchyme culture medium (Yang et al., 1998). This is Minimal Essential Medium (MEM) (Mediatech, VA) containing nonessential amino acids, 100 U/ml penicillin, 100 μg/ml streptomycin, 0.29 mg/ml L-glutamine, and 10% fetal bovine serum (Summit Biotechnology, Fort Collins, CO). In some cases, a single whole lobe (mesenchyme + endoderm) was cultured as a control. Cultures were incubated in 95% air/5% CO_2 at 37°C for a total of 72 h and fixed for 5 min in 4% paraformaldehyde in PBS at 4°C before X-gal staining and further processing.

For recombinations, mesenchyme from single heterozygous *Nog*^{lacZ}/+ lungs was collected and cultured as above. After 24 h, freshly isolated E11.5 wildtype endoderm was placed adjacent to the mesenchyme and cultured for an additional 48 h.

Varying concentrations of recombinant, octyl modified N-Shh (a generous gift of Curis, Inc., Cambridge, MA) were added at the start of culture, either to the medium or loaded on beads. Fgf-loaded beads were added 24 h after the start of culture.

To determine cell numbers, explants were incubated on ice for 15 min in Tyrode–Ringer's solution (Hogan et al., 1994), then for 15 min in 0.25% trypsin–EDTA (Gibco-BRL) at 37°C. After adding an equal volume of Shuger's medium, a single cell suspension was obtained by gentle agitation and cells counted using a hemocytometer. Mean differences between the log numbers of cells/ml in treatments were examined by an analysis of variance procedure, and additionally, an adjustment for multiple comparisons was applied. The results were still statistically significant after adjustment using the Tukey multiple comparisons procedure. This analysis was performed by using the SAS (SAS Inc., Cary, NC) system, version 8.1.

For cell proliferation assays, 5-bromo-2′-deoxyuridine and 5-fluoro-2′-deoxyuridine (Amersham, Buckingshire, England) was added at a 1:1000 dilution after 64 h. Explants were rinsed and fixed after 72 h of culture, and labeled cells were detected with the Cell Proliferation Kit (Amersham), except using fluorescent conjugated secondary antibodies (see below).

Preparation of protein loaded beads

For delivery of Fgf, acrylic beads with immobilized heparin (Sigma H-5263) were rinsed with PBS three times. Beads of approximately 125–175 μm in diameter were placed in siliconized tubes (25 beads/tube) and rotated in 25 ng/μl recombinant human Fgf9 (R&D Systems, Minneapolis, MN), 50 ng/μl recombinant human Fgf10 (generous gift of Dr. Nobuyuki Itoh, or purchased from R&D Systems), or 0.1% BSA for 30 min at 37°C, as described (Kettunen and Thesleff, 1998), and subsequently washed extensively in MEM. Activity of Fgf10 was confirmed by using an endoderm migration assay (Weaver et al., 2000).

For delivery of Shh, Affi-gel Blue Gel beads (100–200 mesh) (Bio-Rad #153-7302, Hercules, CA) were washed and sorted as above and incubated in recombinant, octyl N-Shh (3 or 1 μg/μl) (gift of Curis, Inc.), or 0.1% BSA for 1 h at 37°C.

LacZ activity

Tissues fixed in 4% paraformaldehyde were incubated in X-gal substrate solution (Hogan et al., 1994) for 14 h at 37°C. After washing and postfixation, samples were dehydrated in an isopropanol series, embedded in paraffin, and sectioned at 7 μm. Histoclear (National Diagnostics, Atlanta, GA) was used for embedding and dewaxing.

Immunohistochemistry

Immunohistochemistry was performed on paraffin-embedded sections of intact lungs or explants fixed in 4%

paraformaldehyde. Some of these samples were previously stained for lacZ activity as above. Immunohistochemical reactions were carried out in parallel with control reactions lacking primary antibodies.

Immunofluorescence

Primary antibodies used include: mouse monoclonal anti-α smooth muscle actin (sma) (clone 1A4) (Sigma, St. Louis, MO), at 1:200 or 1:400 dilution and incubated at room temperature for 1 h; rabbit polyclonal anti-smooth muscle myosin (Biomedical Technologies, Inc., Stoughton, MA) at 1:100 dilution after antigen retrieval with 20 μg/ml proteinase K at room temperature for 5 min; rabbit polyclonal anti-phospho-Histone H3 (Upstate Biotechnology, Lake Placid, NY) at 1:1000 dilution incubated at room temperature overnight after microwave antigen retrieval with 10 mM sodium citrate; polyclonal rabbit anti-human pan cytokeratin (Dako, Carpinteria, CA) at 1:500 dilution after proteinase K treatment as above. With the exception of sma, primary antibodies were incubated at 4°C overnight. Cy2 and Cy3 fluorescent conjugated antibodies from Jackson ImmunoResearch (West Grove, PA) were used according to the manufacturer's instructions. Secondary incubations were at room temperature for 1 h. Tissue was counterstained in 0.1 μg/ml DAPI at room temperature for 5 min.

Immunochromagen

Immunostaining for Pecam/CD31 on paraformaldehyde-fixed, paraffin-embedded sections was performed essentially as described (Kalinichenko et al., 2001a). Briefly, slides were treated with 1% trypsin in PBS for 5 min at 37°C to retrieve antigen, then incubated with rat monoclonal anti-pecam antibody (clone MEC13.3) (BD PharMingen, #550274) at a 1:50 dilution overnight at 4°C. Secondary antibody was biotinylated donkey anti-rat (Jackson ImmunoResearch) at 1:200 dilution for 1 h at room temperature. Signal was amplified by using streptavidin–horseradish peroxidase conjugate (Vectastain Elite ABC Kit; Vector, Burlingame, CA) and visualized with 3,3′-diaminobenzidine substrate (Vector). Tissues were counterstained with eosin.

Radioactive in situ hybridization

^{35}S-labeled anti-sense and sense riboprobes were prepared by using the Boehringer Mannheim RNA labeling kit and 850-bp *Fgf9* (Colvin et al., 1999) and 841-bp *Ptc* (Platt et al., 1997) cDNA templates. All probes were hybridized in 50% formamide hybridization mix (Hogan et al., 1994), except those for *Fgf9*, which were hybridized in 55% formamide to decrease background. Slides were exposed to emulsion for 2 (*Ptc*) or 4 (*Fgf9*) days and counterstained with hematoxylin. Twenty-four-hour fixation of explants was required for detection of *Fgf9* in the mesothelium.

Scanning electron microscopy

Explants cultured for 72 h were fixed in 2% glutaraldehyde in phosphate buffer. Controls were accessory lobes from lungs exposed to the same conditions as explants, including pancreatin–trypsin treatment. Samples were rinsed for 5 min in PBS, pH 7.4, after which they were postfixed in 1% buffered osmium tetroxide for 30 min, rinsed with distilled water, and dehydrated in a graded series of ethanol. The samples were dried in a Balzer 020 critical point drying unit by using bone dry CO_2. After mounting on aluminum stubs and gold coating in a Pelco SC-6 sputter coater, samples were viewed in a Hitachi s-2700 scanning electron microscope. Images were acquired digitally by using the Hitachi Quartz PCI imaging system.

Results

Temporal and spatial patterns of expression of Nog^{lacZ}, $Bmp4^{lacZ}$, and Ptc in lung mesenchyme

As a prerequisite to the analysis of lung mesenchyme development, we first established the precise spatial patterns of expression of several important signaling genes transcribed in this tissue, including $Bmp4^{lacZ}$, Nog^{lacZ}, and *Ptc* (Bellusci et al., 1996; Brunet et al., 1998; Lawson et al., 1999; McMahon et al., 1998; Weaver et al., 1999). As shown in Figs. 1 and 2, $Bmp4^{lacZ}$ and Nog^{lacZ} are active in overlapping but not identical domains of lung mesoderm. At E11.5, $Bmp4^{lacZ}$ activity is seen in a wide swath of cells, with highest levels adjacent to the proximal epithelium and lower levels toward the periphery (Fig. 1A–D). At the same stage, strong Nog^{lacZ} expression is restricted to one or two cell layers immediately adjacent to the proximal epithelium (Fig. 1E–G). In addition, Nog^{lacZ}-positive cells are scattered throughout most of the distal mesoderm; these cells appear to express low levels of *Nog*, since their visualization requires long periods of staining and the Xgal product is punctate (Fig. 1H; see also Fig. 2C, E, and J). These overall expression patterns are maintained at E13.5 (Fig. 1I–N), and *Nog*-positive cells are also visible at this time in the developing cartilage rings around the trachea and primary bronchi (Fig. 1M).

The location of Nog^{lacZ}-positive cells adjacent to the proximal endoderm suggested that they are parabronchial smooth muscle (Tollet et al., 2001). This hypothesis was confirmed by colocalization in tissue sections of high levels of β-galactosidase activity and sma in these cells, at all stages examined (E11.5, E13.5, E14.5, E15.5) (Fig. 2C–H, and data not shown). By contrast, Nog^{lacZ} is neither expressed in perivascular smooth muscle (pericytes) associated with blood vessels and capillary beds, nor in the Pecam-expressing endothelial cells themselves (Fig. 2G–J).

The domain of $Bmp4^{lacZ}$ expression includes sma-positive cells adjacent to the endoderm, but also extends beyond it (Fig. 2A and B). Differentiated parabronchial smooth muscle therefore coexpresses $Bmp4^{lacZ}$ and Nog^{lacZ}, at least during the pseudoglandular stage of lung development.

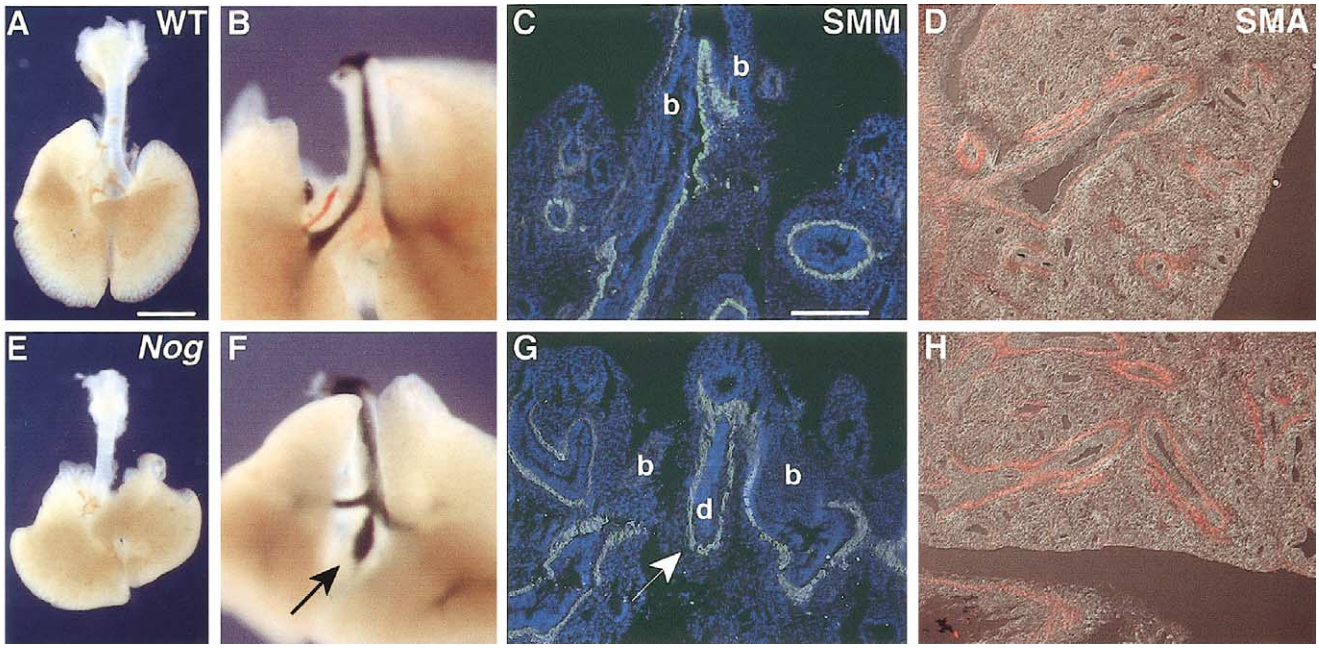

3

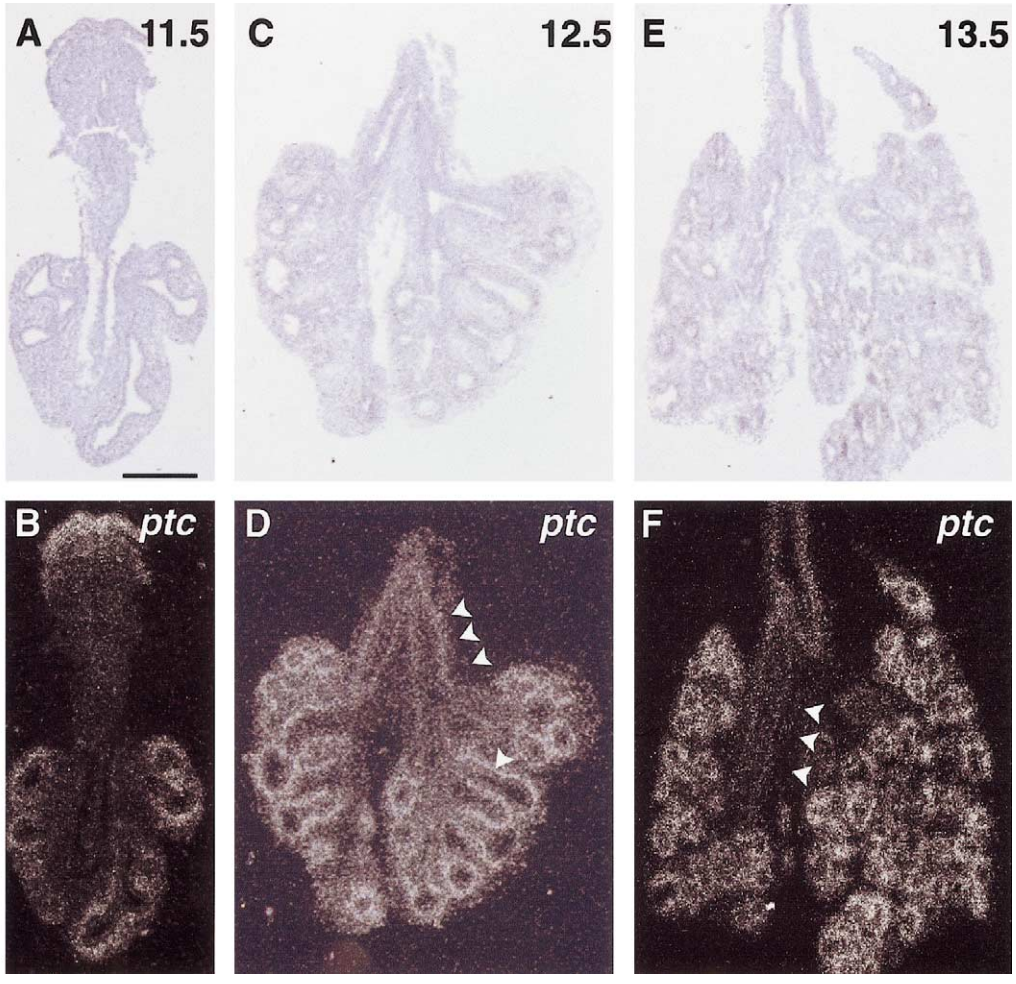

4

Fig. 3. *Nog* mutant lung phenotype. Ventral view of wild-type (A) and *Nog*$^{-/-}$ (E) lungs at E15.5. All *Nog*$^{-/-}$ lungs examined have abnormal gross morphology, with malformed and truncated lobes (E). Dorsal view of E15.5 wild-type (B) and mutant (F) lungs injected with India ink. An ectopic bud is evident between the two main bronchi in the mutant (arrow). Smooth muscle myosin immunostaining (green) and DAPI nuclear staining (blue) of wild-type (C) and mutant (G) lungs at E13.5. A central diverticulum (d) surrounded by smooth muscle is observed between the main bronchi (b) in the mutant. Sma immunostaining (red) and Nomarksi bright-field of wild-type (D) and mutant (H) E15.5 lungs. Smooth muscle differentiation appears normal in the mutant lung. Bar in (A) 1 mm in (A, E); 600 μm in (B, F); Bar in (C), 200 μm in (C, D, G, H).

Fig. 4. *Patched* expression in lung. In situ hybridization in E11.5 lung. (A, B) *Ptc* is expressed in distal mesenchyme surrounding endodermal buds. At E12.5 (C, D), *Ptc* transcripts are high in distal mesenchyme and lower around more proximal airways (single arrowhead) and main bronchi (three arrowheads). At E13.5 (E, F), *Ptc* transcripts are high distally and at lower levels along the main bronchi (arrowheads). Scale bar in (A), 250 μm for (A–F).

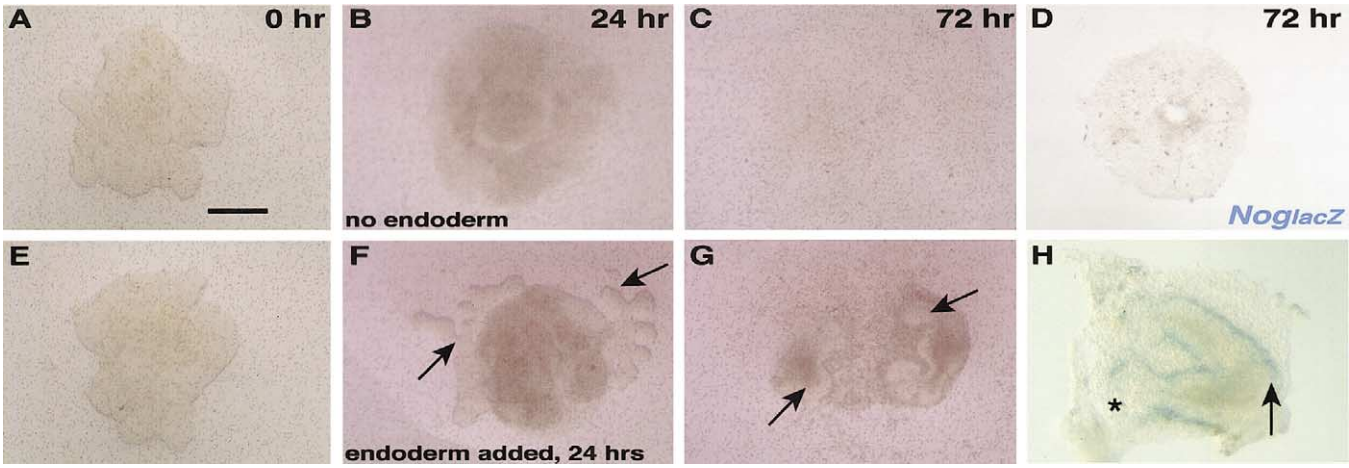

Fig. 5. Endoderm promotes survival and gene expression in lung mesenchyme. Isolated Nog^{lacZ}+/− mesenchyme becomes granular and disintegrates over 72 h of culture (A–C), and Nog^{lacZ}-expressing cells are not maintained (D). When isolated wildtype endoderm (arrows) is added to the cultures after 24 h (F), endodermal and mesenchymal components rapidly reassociate and endoderm (arrows) branches within the mesenchyme (G). Nog^{lacZ}-positive mesenchymal cells are present adjacent to endoderm (H). Note that these cells are detected in proximal regions of the endoderm (arrow) but not surrounding the extending distal tip (asterisk), as observed in vivo (Fig. 2). Scale bar is 400 μm in (A–C, E–G); 300 μm in (D); and 200 μm in (H).

Given the high expression of Nog^{lacZ} in parabronchial smooth muscle, we examined the phenotype of these cells in *Nog* homozygous null embryos. All the lungs of these embryos examined ($n = 30$) exhibited abnormal gross morphology with malformed and truncated lobes (Fig. 3A and B, E and F). Seventy-eight percent (22/28) had fusions of the right lobes, with varying degrees of severity (data not shown), while 31% (9/29) had a blind-ended ectopic bud or diverticulum emerging near the junction of the main bronchi (Fig. 3F and G). However, smooth muscle actin and myosin immunostaining (Fig. 3C and D, G and H) and transmission electron microscopy (data not shown) did not detect abnormalities in the smooth muscle cells associated with proximal airways.

It has been reported by several groups that *Ptc*, which encodes both a receptor for Shh and a transcriptional target of Shh signaling, is transcribed at high levels in the distal lung mesenchyme (Bellusci et al., 1997; Litingtung et al., 1998; Motoyama et al., 1998; Pepicelli et al., 1998). These studies had reported expression at E11.5 but had not examined later stages. Our data (Fig. 4) confirm the high levels of *Ptc* transcript in distal mesenchyme at E11.5 and show that they are maintained at E12.5 and E13.5 (Fig. 4A–F). In addition, however, lower levels of *Ptc* transcript are evident surrounding more proximal airways at both later stages. For example, at E12.5, strong *Ptc* signal is detected around proximal airways and the main bronchi (Fig. 4D, white arrows), while low levels can also be detected along the main bronchus at E13.5 (Fig. 4F, white arrows). Thus, cells throughout the lung mesenchyme, including putative smooth muscle cells around more proximal airways, may be responding to Shh signal in vivo.

Endoderm is required for mesenchymal cell proliferation and Noggin and Bmp4 expression in vitro

Previous studies determined that endoderm of E11.5 lungs produces factors required for the morphogenesis and differentiation of the mesenchyme (Gebb and Shannon, 2000; Taderera, 1967). We confirmed this by culturing isolated distal endoderm and mesoderm in the presence of 10% serum (Fig. 5). Under these conditions, mesenchyme alone spreads as a thin layer over the filter (Fig. 5A–C), and the cells express neither Nog^{lacZ} ($n = 10$) (Figs. 5D and 6A) nor $Bmp4^{lacZ}$ ($n = 14$) (Fig. 6E) after 72 h of culture. Since mesenchyme initially expresses both of these reporters (Fig. 1), this loss of expression is due to either death of the expressing cells or shutoff of gene transcription. If wildtype (+/+) endoderm is added after 24 h, the endoderm and mesenchyme reassociate and the endoderm branches within the mesenchyme (Fig. 5F and G). Moreover, the mesenchymal cells immediately adjacent to the endoderm express Nog^{lacZ}, presumably in smooth muscle cells (Fig. 5H; $n =$ 3/4 lacZ-positive at 48 h; $n = 12/12$ lacZ-positive at 72 h). The *lacZ* activity in these cells verifies that they are derived from the cultured mesenchyme and not from any wildtype mesenchyme carried over with the endoderm. As a control, whole accessory lobes from Nog^{lacZ}+/− lungs consistently express localized Nog^{lacZ} at both 48 h ($n = 5/5$) and 72 h ($n = 13/13$) (data not shown). These results confirm that lung endoderm can maintain the survival of the mesenchyme and further suggest that factor(s) from the endoderm either induce Nog^{lacZ} expression, or promote the survival of Nog^{lacZ}-expressing cells, or both.

Proliferation in response to Shh

We next asked whether recombinant N-Shh protein can substitute for endoderm in the explant system. Explants exposed to increasing doses of Shh are shown in Fig. 6A–D. If Shh is added to the culture medium at 300 ng/ml ($n = 12$), 1 μg/ml ($n = 3$), and 3 μg/ml ($n = 44$), the number of cells increases in a dose-dependent manner compared with controls. Before culture, mesenchyme explants contain, on av-

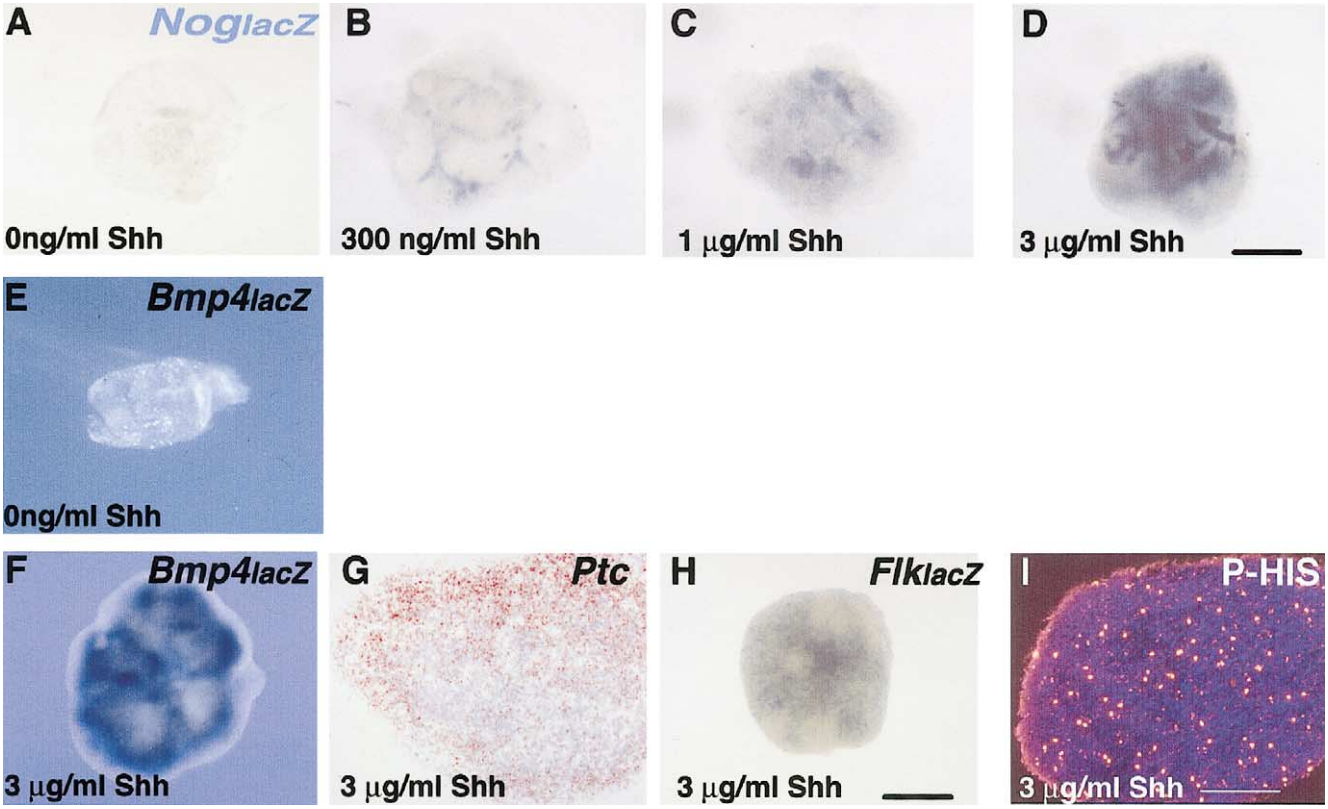

Fig. 6. Dose-dependent growth and gene expression in Shh-treated explants. $Nog^{lacZ}+/-$ lung mesenchyme cultured for 72 h without N-Shh forms a thin layer of cells (A). With 300 ng/ml (B), 1 μg/ml (C), or 3 μg/ml (D) of N-Shh, explants survive and proliferate, and increasing levels of Nog^{lacZ} activity are observed. Explants cultured for 72 h without N-Shh exhibit no $Bmp4^{lacZ}$ activity (E). Explants cultured in 3 μg/ml Shh show expression of $Bmp4^{lacZ}$ (F), *Ptc* (G), and $Flk1^{lacZ}$ (H). Immunostaining of explants for phospho-histone H3 (red), counterstained with DAPI (blue) (I) illustrates proliferation throughout the explant. Scale bars in (D, H), 400 μm for (A–F, H); in (I), 200 μm for (G, I).

erage, 3.7×10^5 cells/ml ($\pm 9.8 \times 10^4$, $n = 6$). By 72 h in the absence of Shh, the cell number declines eightfold, to 4.6×10^4/ml ($\pm 2.2 \times 10^4$, $n = 6$). In contrast, with addition of 300 ng/ml Shh, the average number of cells increases threefold to 1.2×10^6/ml ($\pm 1.8 \times 10^5$, $n = 6$). With 3 μg/ml Shh treatment, an almost ninefold increase is seen, with 3.3×10^6 cells/ml ($\pm 3.8 \times 10^5$, $n = 6$). These numbers are significantly different ($P < 0.0001$; see Materials and methods). Labeling of cultures with BrdU or Phospho-histone H3, a marker of cells in mitosis, shows that proliferating cells are present throughout the explants, including the outer layer and periphery (Fig. 6I; see Fig. 9G and H). Based on these findings, subsequent experiments were carried out with 3 μg/ml Shh in the medium.

Gene expression and cell differentiation in response to Shh

To further assess the response of lung mesenchyme to Shh, we examined gene expression and cellular differentiation. Cultures exposed to 3 μg/ml Shh show high but nonuniform expression of *Ptc* ($n = 4$), Nog^{lacZ} ($n = 24$), and $Bmp4^{lacZ}$ ($n = 7$) throughout the explant (Fig. 6F–H). The increase in Nog^{lacZ} expression was dose-dependent with increasing concentrations of Shh treatment (Fig. 6B–D).

It has been reported that Shh indirectly promotes angiogenesis of blood vessels in vivo (Pola et al., 2001). We therefore examined the effect of N-Shh on the expression of $Flk1^{lacZ}$, a marker of endothelial cells. After 72 h, there are Flk^{lacZ}-positive cells throughout explants treated with 3 μg/ml Shh ($n = 4$) (Fig. 6H). Again, the extent of the staining is dose-dependent, with increasing numbers of Flk^{lacZ}-positive cells observed with increasing concentrations of Shh (data not shown).

Finally, we asked whether the expression of smooth muscle markers is affected by exogenous Shh. As shown in Fig. 7, in the presence of 3 μg/ml Shh, there is strong immunolocalization of both sma and smooth muscle myosin (smm) throughout explants, in a nonuniform pattern. In some regions, there is coincidence between the high Nog^{lacZ} and high sma expression; but in other areas, cells that express high levels of Nog^{lacZ} apparently stain only weakly for sma, and vice versa (compare Fig. 7A and B). This is also the case in vivo, where only a subset of smooth muscle-positive cells also expresses Nog^{lacZ} (see Fig. 2).

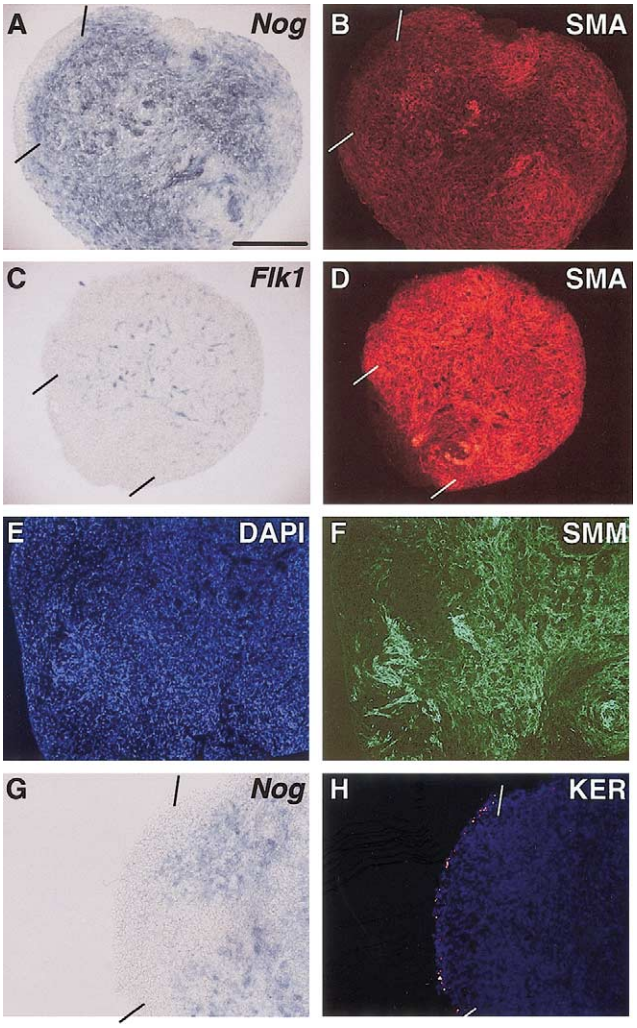

Fig. 7. Gene transcription and cell differentiation in explants cultured for 72 h with 3 μg/ml Shh. (A) Robust Nog^{lacZ} activity throughout a section of an explant culture. Note that expression is absent in some peripheral regions (between black bars). (B) Sma immunostaining of the section in (A). High smooth muscle actin levels are observed throughout the explant, but these regions do not precisely coincide with Nog^{lacZ} expression. Note that sma is absent from the same peripheral regions as *Nog* expression (white bars, see also D). (C–F) Endothelial and smooth muscle cells are both present in explant cultures. (C) Section of $Flk1^{lacZ}+/-$ explant reveals the presence of endothelial cells. Strong sma immunostaining (D) is observed in the explant, but is excluded from $Flk1^{lacZ}$-positive cells. Note that, in some peripheral regions, sma staining and $Flk1^{lacZ}$ activity are both excluded (white and black bars, respectively). Tissue stained with DAPI (E) and antibody to smooth muscle myosin (F) confirms the presence of smooth muscle in explants. (G) A peripheral zone lacking Nog^{lacZ} expression (black bars) is covered with mesothelium, marked by immunostaining for pan-cytokeratin (white bars) (H). Scale bar in (A), 200 μm in (A–D); 100 μm in (G, H).

Lung mesenchyme explants are covered by mesothelium

In mesenchyme explants, we consistently observed zones about five to eight cell diameters wide at the periphery that have low or no expression of Nog^{lacZ}, $Bmp4^{lacZ}$, sma, and $Flk1^{lacZ}$ (Fig. 6F and H; between black bars in Fig. 7A, C, and G and white bars in Fig. 7B and D). We hypothesized that these nonexpressing regions are associated with the mesothelium, a squamous epithelium that covers the outer surface of the embryonic lung in vivo. We tested whether this layer is maintained in vitro using a pan-cytokeratin antibody that stains epithelial cells, including the lung mesothelium, but not mesenchyme. As shown in Fig. 7G and H, wherever mesothelial-like cells are detected in sections of Nog^{lacZ} explants, they are underlain by a domain of low Nog^{lacZ} activity.

To confirm the presence and integrity of mesothelial cells in the culture system, we compared the phenotype of cells on the outer surface of explants with that of normal lung mesothelium. First, histological analysis of sectioned explants shows that the outer cells have a thin, squamous morphology, similar to that of cells covering the E13.5 lung (Fig. 8A and B), and very different from that of the endodermal epithelium, which is cubical or columnar (asterisk, Fig. 8A). This similarity extends to the scanning electron microscope level, where cells on the surface of both explants and normal E11.5 accessory lobes exhibit the characteristic shape and surface microvilli of mesothelial cells (Mutsaers, 2002) (Fig. 8C and D). Finally, cells on the outer surface of explants, like the mesothelium of the normal embryonic lung, express *Fgf9* (Fig. 8E–H; and Colvin et al., 1999).

Fgf9 influences mesenchyme differentiation

Our results suggest that factors released by the mesothelium of explants influence the differentiation of underlying mesenchymal cells. One candidate for mediating this effect, both in vivo and in vitro, is Fgf9. Two potential receptors for this protein, *FgfR1IIIc* and *FgfR2IIIc*, are expressed in lung mesenchyme (Cardoso et al., 1997; Colvin et al., 2001; Orr-Urtreger et al., 1993; Peters et al., 1992). We tested this hypothesis by implanting Fgf9-loaded beads into explants that had been cultured in 3 μg/ml N-Shh for 24 h. Under these conditions, Nog^{lacZ} expression is inhibited around the bead (n = 8/8) (Fig. 9A and C). By contrast, this inhibitory effect is not seen with beads loaded with either PBS (n = 0/10) or Fgf10, a factor which signals through an alternative receptor to Fgf9 (n = 0/7) (Fig. 9B and D). Fgf9-soaked beads also inhibit the differentiation of sma-positive cells (Fig. 9E, n = 13), an effect not seen with Fgf10 (Fig. 9F; n = 7) or PBS beads (data not shown; n = 3). BrdU incorporation studies did not detect any difference in cell proliferation levels surrounding beads loaded with either Fgf9 (Fig. 9G; n = 7) or Fgf10 (Fig. 9H; n = 4). Rather, proliferation appears uniform throughout the explant.

Locally applied Shh upregulates Ptc and Bmp4 in lung mesenchyme explants

To test the local action of Shh, we applied N-Shh-loaded beads to mesenchyme explants. In these cases, the expression of both *Ptc* (Fig. 10A and B) and $Bmp4^{lacZ}$ (n = 13/15) (Fig. 10E and G) is localized around the bead. However,

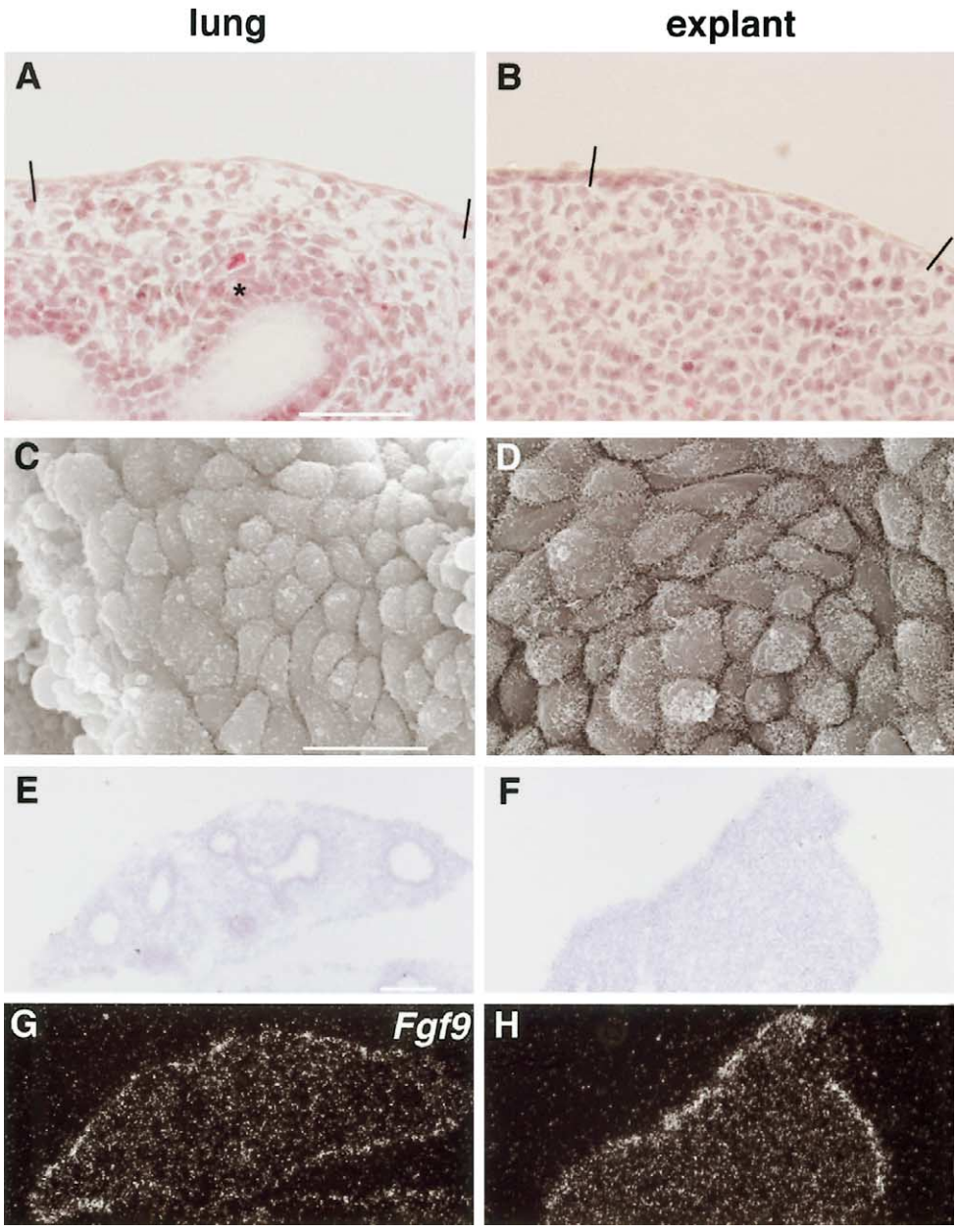

Fig. 8. Characterization of mesothelial cells. Mesothelial cells of the wildtype lung (A) (between black bars) are squamous, contrasting with cuboidal endodermal cells (*). (B) Cells covering a Shh-treated explant (between black bars) exhibit similar squamous morphology. (C) Scanning electron micrograph of an isolated E11.5 accessory lobe shows characteristic mesothelial cells with surface microvilli. (D) Cells with similar morphology on the surface of an explant after 72 h. (E) Hematoxylin-stained E13.5 lung lobe. (F) Hematoxylin-stained explant. (G) *Fgf9* transcript is detected in putative mesothelial cells at the periphery of an E13.5 lung lobe. (H) *Fgf9* transcript is detected at the periphery of the explant. All explants shown were treated with 3 μg/ml Shh. Scale bars in (A), 50 μm in (A, B); in (C), 15 μm in (C, D); in (E), 100 μm in (E–H).

proliferation occurs throughout the explant (Fig. 10C and D). Compared with *Ptc* and $Bmp4^{lacZ}$, a much less uniform distribution of Nog^{lacZ} (Fig. 10F and H; $n = 9/9$) and sma expression (Fig. 10I and J) is seen relative to the Shh-loaded beads, and the two products do not always colocalize. The reason for this result is not clear, but suggests that some responses to a localized source of Shh are particularly sensitive to factors such as local cell density and uneven extracellular matrix accumulation.

Discussion

The patterning and differentiation of the mesenchyme in the developing lung is a largely unexplored area. Here, we have established an explant assay system in which N-Shh can substitute for some of the well-documented functions of the lung endoderm in supporting the survival, proliferation, and differentiation of the mesoderm (Gebb and Shannon, 2000; Taderera, 1967) (Fig. 5). Using this assay, we can, for

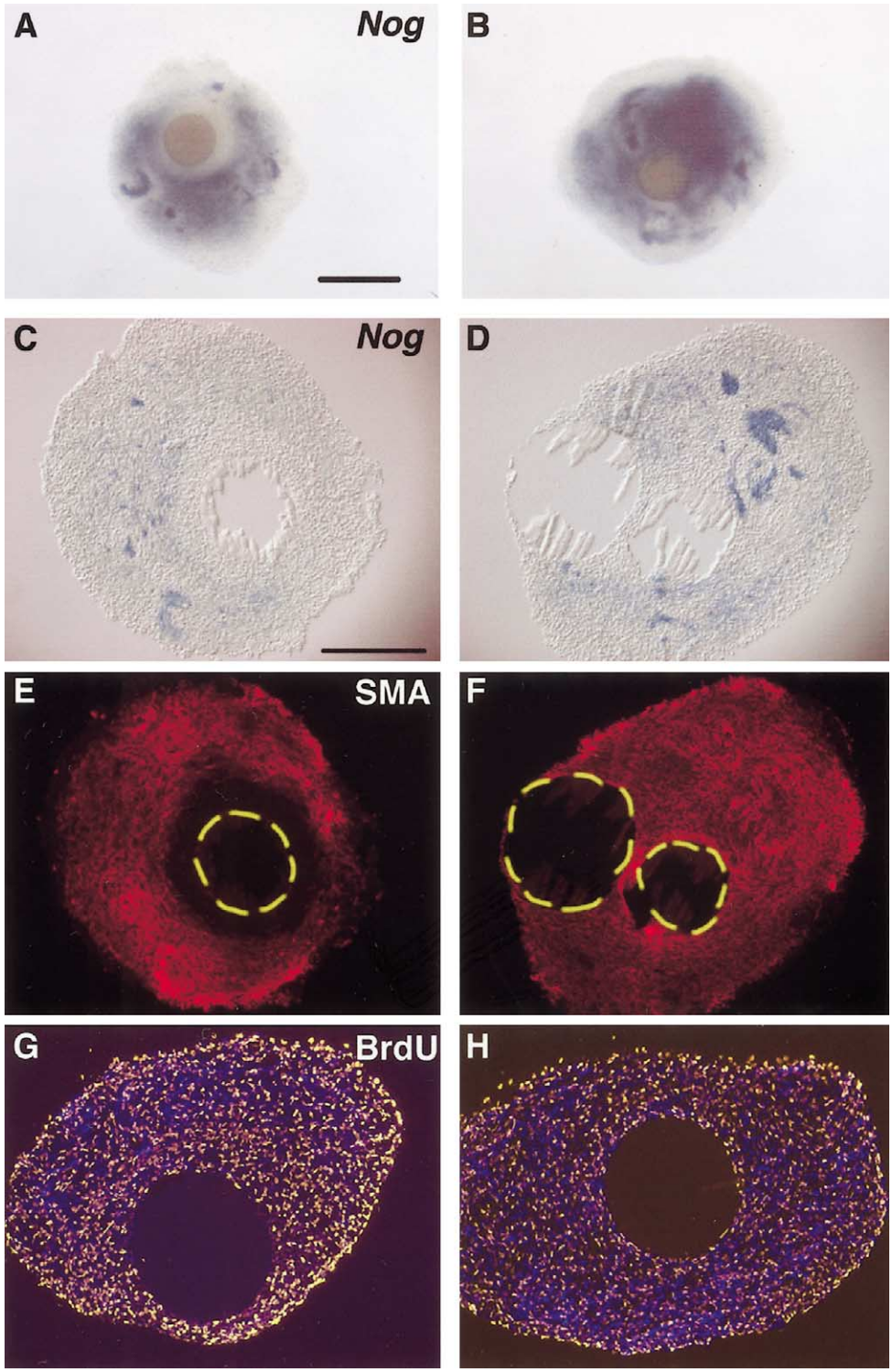

Fig. 9. Fgf9 inhibits *Nog*^{lacZ} transcription and sma levels in Shh-treated explants. A distinct domain of cells lacking *Nog*^{lacZ} activity is observed around an Fgf9-loaded bead implanted into Shh-treated lung mesenchyme (A). A control Fgf10-loaded bead does not affect *Nog*^{lacZ} expression (B). A section from another explant confirms that both *Nog*^{lacZ} expression (C) and sma immunostaining (E) are decreased in a ring of cells surrounding an Fgf9 bead. A section of an explant treated with an Fgf10-loaded control bead shows no effect on the localization of *Nog*^{lacZ} (D) and sma (F)-positive cells adjacent to the bead. Yellow dashed lines indicate bead boundaries. BrdU immunostaining (orange) reveals uniform proliferation throughout the explants and does not detect localized proliferation in response to an Fgf9 (G)- or Fgf10-loaded (H) bead. Counterstaining is DAPI (blue). All explants were treated with 3 μg/ml Shh for 72 h. BrdU labeling was performed for 4 h prior to fixation. Scale bar in (A), 300 μm in (A, B); in (C), 200 μm in (C–H).

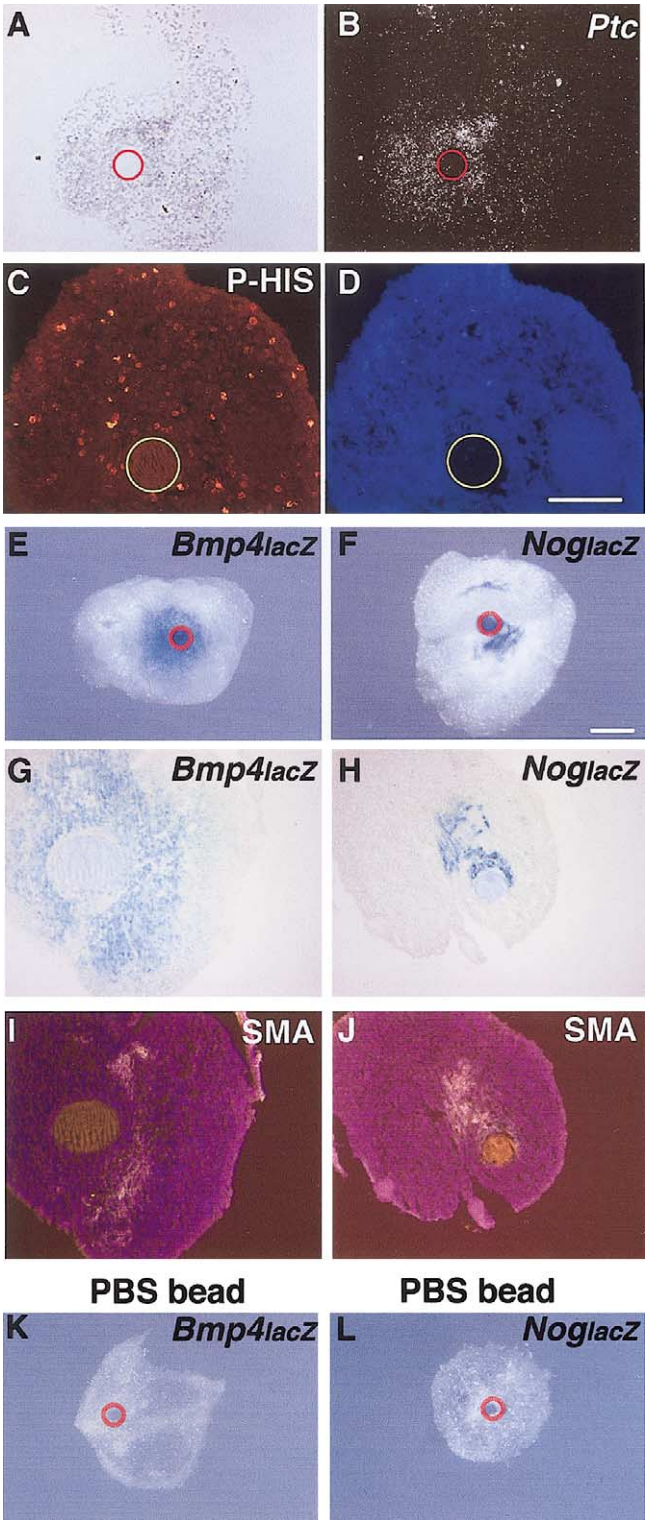

Fig. 10. Shh loaded beads induce localized *Ptc* and $Bmp4^{lacZ}$. (A) *Ptc* expression is detected in a localized domain around the Shh-loaded bead (red circle) in explant culture (B). Phosphohistone H3 antibody staining detects proliferating cells throughout the explant, not centered around the bead (yellow circle) (C). DAPI counterstaining of the explant (D). $Bmp4^{lacZ}$ is induced locally around a Shh-loaded bead (red circles), as viewed both in whole-mount (E) and section (G). Nog^{lacZ}-positive cells are also observed, but are not exclusively localized around the bead in either whole mount (F) or section (H). Costaining of these sections for Sma (orange) reveals that smooth muscle cells are present, but are also not restricted to the region immediately around the bead (I, J). Cells are counterstained with DAPI. Neither $Bmp4^{lacZ}$ (K)- nor Nog^{lacZ} (L)-positive cells are detected in explants cultured with PBS-loaded control beads (red circles). Scale bars in (D), 200 μm for (A, B); 100 μm for (C, D, G, J); in (F), 300 μm for (E, F, K, L).

the first time, manipulate molecular factors in order to assess their direct effects on the mesenchyme. We find that recombinant N-Shh promotes both the proliferation of lung mesenchyme and the differentiation of smooth muscle. By contrast, signals from the mesothelium, particularly Fgf9, inhibit at least some of the effects of N-Shh on mesenchyme differentiation. We conclude that the endoderm and the mesothelium normally work together to regulate the size and fate of a pool of mesenchyme progenitor cells in the distal lung. In the future, modifications of the culture system, including the replacement of serum factors and the identification of cell-autonomous markers for multiple specific mesodermal cell types, will allow these regulatory mechanisms to be further explored.

Effect of Shh on lung mesenchyme differentiation

In vivo or in vitro, the expression of Nog^{lacZ} and sma is tightly restricted to mesenchyme that is in close proximity with lung endoderm, a tissue producing N-Shh (Figs. 1, 2, and 5). By contrast, exogenous N-Shh in the culture medium induces the expression of these markers throughout the mesenchyme, with the exception of a peripheral zone (discussed below). In this assay, the number of cells expressing markers for specific cell types (including Nog^{lacZ} and sma) increases in a dose-dependent manner in response to recombinant protein, illustrating that more mesodermal cells have the potential to express these genes than normally do so in vivo. This suggests that Shh not only supports the survival and proliferation of preexisting cell types but also (directly or indirectly) promotes the differentiation of progenitor cells into specific lineages. Our bead studies further show that *Ptc* and $Bmp4^{lacZ}$ are induced uniformly in the mesenchyme in response to a localized source of Shh (Fig. 10). However, since markers of smooth muscle, such as Nog^{lacZ} and sma, are not induced in a reproducible spatial pattern around the bead, differentiation must be influenced by other factors, such as local cell density and extracellular matrix accumulation (Yang et al., 1999; Zhang et al., 1999). Alternatively, or in addition, Shh may indirectly induce these markers by affecting the expression of other signaling molecules. Among the other factors that have been implicated in promoting smooth muscle differentiation in the lung are members of the platelet-derived growth factor (Pdgf) and transforming growth factor β (Tgfβ) families of signaling molecules (Bostrom et al., 1996; Bragg et al., 2001; Lindahl et al., 1999; Sun et al., 2000; Zhou et al., 1996).

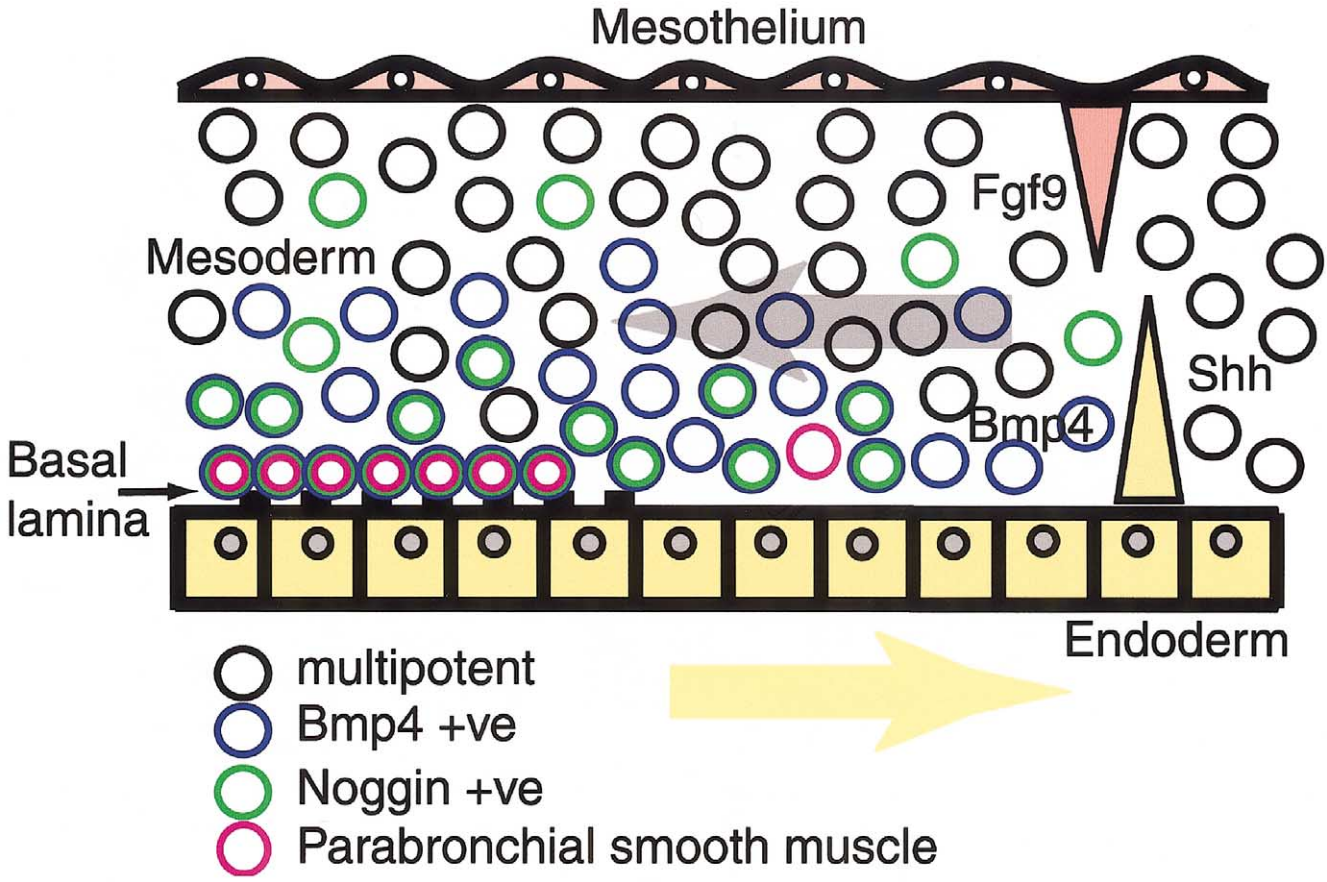

Fig. 11. "Sandwich" model for patterning of lung mesenchyme. Mesenchymal cells (circles) are sandwiched between the mesothelium (pink) and the endoderm (yellow). Signals from the mesothelium, such as Fgf9 (pink triangle), help to maintain peripheral cells in an undifferentiated or multipotent state. Shh made by the endoderm (yellow triangle) promotes cell survival/proliferation, and also induces differentiation. Factors made by the more proximal endoderm, including basal lamina proteins (black dotted line), promote terminal differentiation of parabronchial smooth muscle. Arrows indicate relative movement of mesenchyme (gray) and endoderm (yellow). Open circles, multipotent cells; green circles, *Nog*-expressing cells; blue circles, *Bmp4*-expressing cells; red circles, sma-positive cells. Cells can be positive for *Nog*, *Bmp4*, and sma, or any combination of these markers.

Our results in culture provide evidence that Shh signaling over an extended period promotes the differentiation of lung mesenchyme into smooth muscle. This conclusion is compatible with genetic studies implicating *Shh*, and its downstream target *Foxf1*, in the differentiation of smooth muscle in the normal lung (Kalinichenko et al., 2001b; Lim et al., 2002; Mahlapuu et al., 2001; Pepicelli et al., 1998). However, our results raise an apparent paradox: *Shh* is normally expressed throughout the lung endoderm, with highest levels in the distal tips, and *Ptc* transcription is also highest in the distal mesenchyme, compared with mesenchyme around the proximal endoderm (Fig. 4). Yet, smooth muscle cells are absent from these domains of distal mesoderm. This paradox may be explained by the rapid outgrowth of respiratory endoderm during lung development in vivo. After initial exposure to high levels of Shh at the endoderm tip, the mesenchymal cells may move proximally relative to the distal endoderm. This may be a passive translocation, driven by endoderm outgrowth, and/or involve active mesenchymal cell migration. By the time they are competent to differentiate into smooth muscle, the mesenchyme cells are thus localized around proximal endoderm (Fig. 11). These models will be tested in the future by using lineage labeling techniques.

Endodermal and mesenchymal Bmp4 expression domains are differentially regulated

Our studies reveal differential regulation of *Bmp4* in the endodermal and mesenchymal tissue layers of the lung. The explant experiments provide evidence that Shh, normally made by the endoderm, induces *Bmp4* in lung mesenchyme, at least at early stages of development. This finding is in agreement with reports that *Bmp4* transcripts are lost in *Shh* mutant lung mesenchyme (Litingtung et al., 1998). Moreover, local induction of *Bmp2/4* by Shh has been reported in several other organs, including the hindgut (Roberts et al., 1995; Sukegawa et al., 2000), the pituitary (Treier et al., 2001), and the kidney (Yu et al., 2002). This contrasts with endodermal regulation of *Bmp4* in the lung, which is controlled by localized Fgf signals, including Fgf10, in distal mesenchyme (Hyatt et al., 2002; Lebeche et al., 1999;

Weaver et al., 2000). Taken together, these results emphasize that the same gene, *Bmp4*, can be regulated by different signals in adjacent cell populations. It is also likely that there are stage-specific changes in the response of lung mesenchyme to Shh, since our previous studies of transgenic embryos overexpressing Shh in lung endoderm showed no change in the expression of *Bmp4* in the lung at E18.5 (Bellusci et al., 1997).

Factors made by the mesothelium regulate mesenchyme differentiation

The mesothelium expresses high levels of *Fgf9* from the early pseudoglandular stage, and $Fgf9^{-/-}$ lungs are smaller than wild type (Colvin et al., 2001). Despite extensive analysis, no missing cell types or other differentiation defects are detected in these lungs. It has therefore been suggested that Fgf9 from the mesothelium functions to maintain the proliferation of distal mesenchyme, including cells that express *Fgf10* (Colvin et al., 2001). Our data support this hypothesis and provide further novel evidence that Fgf9 counteracts factors, including Shh, that promote the differentiation of the mesenchyme. We hypothesize that mesenchymal progenitor cells in the periphery of the developing lung, exposed to high levels of Fgf9 and relatively low levels of Shh, are maintained in an undifferentiated state (Fig. 11). However, we cannot rule out the possibility that Fgf9 promotes their differentiation into peripheral mesenchymal cell types for which we do not yet have markers. The differentiation state of the mesenchyme may be further modulated by other factors made by the mesothelium, such as Tgfβ3 (Bragg et al., 2001; Pelton et al., 1991) and retinoic acid (Malpel et al., 2000; Niederreither et al., 2002).

Conclusion: "sandwich" model for the patterning of mesenchyme during early lung development

In summary, we propose the following model for lung mesenchyme development, as depicted in Fig. 11:

In the early lung, mesenchyme is "sandwiched" between two distinct tissues: the endoderm and the mesothelium. From the interior of the lung, Shh produced by the endoderm promotes the proliferation of the mesenchyme, possibly by acting as a direct mitogen and modulating the levels of intracellular cyclins (Barnes et al., 2001; Duman-Scheel et al., 2002; Long et al., 2001). In addition, Shh may have roles in controlling cell fate and cell differentiation. However, whether it acts directly as a morphogen, as in the vertebrate neural tube (for review, see Marti and Bovolenta, 2002), or indirectly by inducing mesenchymal factors such as Bmp4, remains an open question. Toward the periphery, the cells come under the influence of the mesothelium, which inhibits stromal cell differentiation and thereby helps to maintain a local population of multipotent progenitor cells. Fgf9 plays an important role in this process. Future studies will be directed at identifying molecular markers for mesenchymal progenitor populations and at clarifying how signals from both the endoderm and mesothelium regulate differentiation and patterning.

Acknowledgments

Recombinant N-Shh was generously donated by Curis, Inc. We thank R. Harland for Nog^{lacZ} mice, T. Daniel for $Flk1^{lacZ}$ mice, members of the L. Solnica-Krezel lab for imaging assistance, B. LaFleur for statistical analysis, and B. Fegley of the Electron Microscopy Research Laboratory at Kansas University Medical Center for scanning electron microscopy. We thank S.K. Dey, D. Bader, and members of the C. Wright and Hogan labs for discussion, and especially H. Kulessa for his invaluable insight. This work was supported by HD28955. B.L.M.H is an Investigator of the Howard Hughes Medical Institute.

References

Barnes, E.A., Kong, M., Ollendorff, V., Donoghue, D.J., 2001. Patched 1 interacts with cyclin B1 to regulate cell cycle progression. EMBO J. 20, 2214–2223.

Bellusci, S., Furuta, Y., Rush, M.G., Henderson, R., Winnier, G., Hogan, B.L.M., 1997. Involvement of Sonic hedgehog (Shh) in mouse embryonic lung growth and morphogenesis. Development 124, 53–63.

Bellusci, S., Henderson, R., Winnier, G., Oikawa, T., Hogan, B.L.M., 1996. Evidence from normal expression and targeted misexpression that bone morphogenetic protein (Bmp-4) plays a role in mouse embryonic lung morphogenesis. Development 122, 1693–1702.

Bitgood, M.J., McMahon, A.P., 1995. Hedgehog and Bmp genes are coexpressed at many diverse sites of cell- cell interaction in the mouse embryo. Dev. Biol. 172, 126–138.

Bostrom, H., Willetts, K., Pekny, M., Leveen, P., Lindahl, P., Hedstrand, H., Pekna, M., Hellstrom, M., Gebre-Medhin, S., Schalling, M., Nilsson, M., Kurland, S., Tornell, J., Heath, J.K., Betsholtz, C., 1996. PDGF-A signaling is a critical event in lung alveolar myofibroblast development and alveogenesis. Cell 85, 863–873.

Bragg, A.D., Moses, H.L., Serra, R., 2001. Signaling to the epithelium is not sufficient to mediate all of the effects of transforming growth factor beta and bone morphogenetic protein 4 on murine embryonic lung development. Mech. Dev. 109, 13–26.

Brunet, L.J., McMahon, J.A., McMahon, A.P., Harland, R.M., 1998. Noggin, cartilage morphogenesis, and joint formation in the mammalian skeleton. Science 280, 1455–1457.

Cardoso, W.V., 2001. Molecular regulation of lung development. Annu. Rev. Physiol. 63, 471–494.

Cardoso, W.V., Itoh, A., Nogawa, H., Mason, I., Brody, J.S., 1997. FGF-1 and FGF-7 induce distinct patterns of growth and differentiation in embryonic lung epithelium. Dev. Dyn. 208, 398–405.

Colvin, J.S., Feldman, B., Nadeau, J.H., Goldfarb, M., Ornitz, D.M., 1999. Genomic organization and embryonic expression of the mouse fibroblast growth factor 9 gene. Dev. Dyn. 216, 72–88.

Colvin, J.S., White, A.C., Pratt, S.J., Ornitz, D.M., 2001. Lung hypoplasia and neonatal death in Fgf9-null mice identify this gene as an essential regulator of lung mesenchyme. Development 128, 2095–2106.

deMello, D.E., Sawyer, D., Galvin, N., Reid, L.M., 1997. Early fetal development of lung vasculature. Am. J. Respir. Cell Mol. Biol. 16, 568–581.

Duman-Scheel, M., Weng, L., Xin, S., Du, W., 2002. Hedgehog regulates cell growth and proliferation by inducing Cyclin D and Cyclin E. Nature 417, 299–304.

Gebb, S.A., Shannon, J.M., 2000. Tissue interactions mediate early events in pulmonary vasculogenesis. Dev. Dyn. 217, 159–169.

Grindley, J.C., Bellusci, S., Perkins, D., Hogan, B.L., 1997. Evidence for the involvement of the Gli gene family in embryonic mouse lung development. Dev. Biol. 188, 337–348.

Hall, S.M., Hislop, A.A., Pierce, C.M., Haworth, S.G., 2000. Prenatal origins of human intrapulmonary arteries: formation and smooth muscle maturation. Am. J. Respir. Cell Mol. Biol. 23, 194–203.

Hogan, B.L.M., Beddington, R., Costantini, F., Lacy, E., 1994. Manipulating the Mouse Embryo. Cold Spring Harbor Press, Cold Spring Harbor, NY.

Hogan, B.L.M., Grindley, J., Bellusci, S., Dunn, N.R., Emoto, H., Itoh, N., 1997. Branching morphogenesis of the lung: new models for a classical problem. Cold Spring Harbor Symp. Quant. Biol. 62, 249–256.

Hui, C.C., Slusarski, D., Platt, K.A., Holmgren, R., Joyner, A.L., 1994. Expression of three mouse homologs of the Drosophila segment polarity gene cubitus interruptus, Gli, Gli-2, and Gli-3, in ectoderm- and mesoderm-derived tissues suggests multiple roles during postimplantation development. Dev. Biol. 162, 402–413.

Hyatt, B.A., Shangguan, X., Shannon, J.M., 2002. BMP4 modulates fibroblast growth factor-mediated induction of proximal and distal lung differentiation in mouse embryonic tracheal epithelium in mesenchyme-free culture. Dev. Dyn. 225, 153–165.

Kalinichenko, V.V., Lim, L., Shin, B., Costa, R.H., 2001a. Differential expression of forkhead box transcription factors following butylated hydroxytoluene lung injury. Am. J. Physiol. Lung Cell Mol. Physiol. 280, L695–L704.

Kalinichenko, V.V., Lim, L., Stolz, D.B., Shin, B., Rausa, F.M., Clark, J., Whitsett, J.A., Watkins, S.C., Costa, R.H., 2001b. Defects in pulmonary vasculature and perinatal lung hemorrhage in mice heterozygous null for the Forkhead Box f1 transcription factor. Dev. Biol. 235, 489–506.

Kapanchi, Y., Gabbiani, G., 1997. Contractile cells in pulmonary alveolar tissue, in: Crystal, R.G., West, J.B., Weibel, E.R., Barnes, P.J. (Eds.), The Lung: Scientific Foundations, Lippincott-Raven Publishers, Philadelphia, pp. 697–707.

Kettunen, P., Thesleff, I., 1998. Expression and function of FGFs-4, and -8, and -9 suggest functional redundancy and repetitive use as epithelial signals during tooth morphogenesis. Dev. Dyn. 211,, 256–268.

Lawson, K.A., Dunn, N.R., Roelen, B.A., Zeinstra, L.M., Davis, A.M., Wright, C.V., Korving, J.P., Hogan, B.L., 1999. Bmp4 is required for the generation of primordial germ cells in the mouse embryo. Genes Dev. 13, 424–436.

Lebeche, D., Malpel, S., Cardoso, W.V., 1999. Fibroblast growth factor interactions in the developing lung. Mech. Dev. 86, 125–136.

Lim, L., Kalinichenko, V.V., Whitsett, J.A., Costa, R.H., 2002. Fusion of lung lobes and vessels in mouse embryos heterozygous for the forkhead box f1 targeted allele. Am. J. Physiol. Lung Cell Mol. Physiol. 282, L1012–L1022.

Lindahl, P., Bostrom, H., Karlsson, L., Hellstrom, M., Kalen, M., Betsholtz, C., 1999. Role of platelet-derived growth factors in angiogenesis and alveogenesis. Curr. Top. Pathol. 93, 27–33.

Litingtung, Y., Lei, L., Westphal, H., Chiang, C., 1998. Sonic hedgehog is essential to foregut development. Nat. Genet. 20, 58–61.

Long, F., Zhang, X.M., Karp, S., Yang, Y., McMahon, A.P., 2001. Genetic manipulation of hedgehog signaling in the endochondral skeleton reveals a direct role in the regulation of chondrocyte proliferation. Development 128, 5099–5108.

Mahlapuu, M., Enerback, S., Carlsson, P., 2001. Haploinsufficiency of the forkhead gene Foxf1, a target for sonic hedgehog signaling, causes lung and foregut malformations. Development 128, 2397–2406.

Malpel, S., Mendelsohn, C., Cardoso, W.V., 2000. Regulation of retinoic acid signaling during lung morphogenesis. Development 127, 3057–3067.

Marti, E., Bovolenta, P., 2002. Sonic hedgehog in CNS development: one signal, multiple outputs. Trends Neurosci. 25, 89–96.

McGowan, S.E., Torday, J.S., 1997. The pulmonary lipofibroblast (lipid interstitial cell) and its contributions to alveolar development. Annu. Rev. Physiol. 59, 43–62.

McMahon, J.A., Takada, S., Zimmerman, L.B., Fan, C.M., Harland, R.M., McMahon, A.P., 1998. Noggin-mediated antagonism of BMP signaling is required for growth and patterning of the neural tube and somite. Genes Dev. 12, 1438–1452.

Miller, L.A., Wert, S.E., Whitsett, J.A., 2001. Immunolocalization of sonic hedgehog (Shh) in developing mouse lung. J. Histochem. Cytochem. 49, 1593–1604.

Motoyama, J., Liu, J., Mo, R., Ding, Q., Post, M., Hui, C.C., 1998. Essential function of Gli2 and Gli3 in the formation of lung, trachea and oesophagus. Nat. Genet. 20, 54–57.

Mutsaers, S.E., 2002. Mesothelial cells: their structure, function and role in serosal repair. Respirology 7, 171–191.

Niederreither, K., Fraulob, V., Garnier, J.M., Chambon, P., Dolle, P., 2002. Differential expression of retinoic acid-synthesizing (RALDH) enzymes during fetal development and organ differentiation in the mouse. Mech. Dev. 110, 165–171.

Orr-Urtreger, A., Bedford, M.T., Burakova, T., Arman, E., Zimmer, Y., Yayon, A., Givol, D., Lonai, P., 1993. Developmental localization of the splicing alternatives of fibroblast growth factor receptor-2 (FGFR2). Dev. Biol. 158, 475–486.

Park, H.L., Bai, C., Platt, K.A., Matise, M.P., Beeghly, A., Hui, C.C., Nakashima, M., Joyner, A.L., 2000. Mouse Gli1 mutants are viable but have defects in SHH signaling in combination with a Gli2 mutation. Development 127, 1593–1605.

Partanen, J., Puri, M.C., Schwartz, L., Fischer, K.D., Bernstein, A., Rossant, J., 1996. Cell autonomous functions of the receptor tyrosine kinase TIE in a late phase of angiogenic capillary growth and endothelial cell survival during murine development. Development 122, 3013–3021.

Pelton, R.W., Johnson, M.D., Perkett, E.A., Gold, L.I., Moses, H.L., 1991. Expression of transforming growth factor-beta 1, -beta 2, and -beta 3 mRNA and protein in the murine lung. Am. J. Respir. Cell Mol. Biol. 5, 522–530.

Pepicelli, C.V., Lewis, P.M., McMahon, A.P., 1998. Sonic hedgehog regulates branching morphogenesis in the mammalian lung. Curr. Biol. 8, 1083–1086.

Peters, K.G., Werner, S., Chen, G., Williams, L.T., 1992. Two FGF receptor genes are differentially expressed in epithelial and mesenchymal tissues during limb formation and organogenesis in the mouse. Development 114, 233–243.

Platt, K.A., Michaud, J., Joyner, A.L., 1997. Expression of the mouse Gli and Ptc genes is adjacent to embryonic sources of hedgehog signals suggesting a conservation of pathways between flies and mice. Mech. Dev. 62, 121–135.

Pola, R., Ling, L.E., Silver, M., Corbley, M.J., Kearney, M., Blake Pepinsky, R., Shapiro, R., Taylor, F.R., Baker, D.P., Asahara, T., Isner, J.M., 2001. The morphogen Sonic hedgehog is an indirect angiogenic agent upregulating two families of angiogenic growth factors. Nat. Med. 7, 706–711.

Roberts, D.J., Johnson, R.L., Burke, A.C., Nelson, C.E., Morgan, B.A., Tabin, C., 1995. Sonic hedgehog is an endodermal signal inducing Bmp-4 and Hox genes during induction and regionalization of the chick hindgut. Development 121, 3163–3174.

Shalaby, F., Rossant, J., Yamaguchi, T.P., Gertsenstein, M., Wu, X.F., Breitman, M.L., Schuh, A.C., 1995. Failure of blood-island formation and vasculogenesis in Flk-1-deficient mice. Nature 376, 62–66.

Sukegawa, A., Narita, T., Kameda, T., Saitoh, K., Nohno, T., Iba, H., Yasugi, S., Fukuda, K., 2000. The concentric structure of the developing gut is regulated by Sonic hedgehog derived from endodermal epithelium. Development 127, 1971–1980.

Sun, T., Jayatilake, D., Afink, G.B., Ataliotis, P., Nister, M., Richardson, W.D., Smith, H.K., 2000. A human YAC transgene rescues craniofacial and neural tube development in PDGFRalpha knockout mice and uncovers a role for PDGFRalpha in prenatal lung growth. Development 127, 4519–4529.

Taderera, J.V., 1967. Control of lung differentiation in vitro. Dev. Biol. 16, 489–512.

Tollet, J., Everett, A.W., Sparrow, M.P., 2001. Spatial and temporal distribution of nerves, ganglia, and smooth muscle during the early pseudoglandular stage of fetal mouse lung development. Dev. Dyn. 221, 48–60.

Treier, M., O'Connell, S., Gleiberman, A., Price, J., Szeto, D.P., Burgess, R., Chuang, P.T., McMahon, A.P., Rosenfeld, M.G., 2001. Hedgehog signaling is required for pituitary gland development. Development 128, 377–386.

Weaver, M., Dunn, N.R., Hogan, B.L., 2000. Bmp4 and Fgf10 play opposing roles during lung bud morphogenesis. Development 127, 2695–2704.

Weaver, M., Yingling, J.M., Dunn, N.R., Bellusci, S., Hogan, B.L., 1999. Bmp signaling regulates proximal-distal differentiation of endoderm in mouse lung development. Development 126, 4005–4015.

Yang, Y., Palmer, K.C., Relan, N., Diglio, C., Schuger, L., 1998. Role of laminin polymerization at the epithelial mesenchymal interface in bronchial myogenesis. Development 125, 2621–2629.

Yang, Y., Relan, N.K., Przywara, D.A., Schuger, L., 1999. Embryonic mesenchymal cells share the potential for smooth muscle differentiation: myogenesis is controlled by the cell's shape. Development 126, 3027–3033.

Yu, J., Carroll, T.J., McMahon, A.P., 2002. Sonic hedgehog regulates proliferation and differentiation of mesenchymal cells in the mouse metanephric kidney. Development 129, 5301–5312.

Zhang, J., O'Shea, S., Liu, J., Schuger, L., 1999. Bronchial smooth muscle hypoplasia in mouse embryonic lungs exposed to a laminin beta1 chain antisense oligonucleotide. Mech. Dev. 89, 15–23.

Zhou, L., Dey, C.R., Wert, S.E., Whitsett, J.A., 1996. Arrested lung morphogenesis in transgenic mice bearing an SP-C-TGF-beta 1 chimeric gene. Dev. Biol. 175, 227–238.